Numerical study of a positive latent cold storage system for industrial applications: Discharge mode

Y. Khattari, E.H. Sebbar, Y. Chaibi, T.El. Rhafiki, Tarik Kousksou, Y. Zeraouli

Numerical study of a positive latent cold storage system for industrial applications: Discharge mode

Y. Khattari[(a)], E.H.Sebbar [(b)],Y. Chaibi[(a)], T. El Rhafiki[(b)], T. Kousksou[(a)], Y. Zeraouli[(a)]

[(a)] Universite de Pau et des Pays de l'Adour, E2S UPPA, SIAME, Pau, France
[(b)] Engineering Sciences Laboratory, Polydisciplinary Faculty of Taza, Sidi Mohamed Ben Abdellah University Fez Morocco, Morocco

Abstract: In this work, a comprehensive numerical study on a latent heat storage system is presented. The adopted storage system consists of a tank with a fixed bed of phase-change materials (PCMs). A numerical model simulating the dynamic and thermal behaviour of this system during the discharge period has been developed and validated using experimental data from the literature. During the discharge mode, when the inlet heat transfer fluid (HTF) is maintained at a temperature near the melting temperature of the PCM, a quasi-stabilization of the outlet HTF temperature is observed. The duration of the discharged energy is increased when the flowrate of the fluid is decreased. A detailed study was also carried out to better understand the behaviour of latent storage system using multiple PCMs. The obtained results for a multi-PCM configurations reveal that the latent energy released during the discharge period depends on the placement order of the PCMs inside the tank, the flow rate of the HTF and the level temperature of the HTF at the inlet to the tank. This numerical study could a be a key solution in industrial cold applications such as air conditioning and thermal comfort, the medical and food sectors.

Keywords: PCM; Packed bed; Cold storage; Heat transfer; Discharge mode

Nomenclature

A	superficial capsule area [m^{-1}]
c	specific heat capacity [$J.K^{-1}.kg^{-1}$]
d	diameter of capsules [m]
D	diameter of the tank [m]
f	liquid fraction
g	gravitational acceleration [$m.s^{-2}$]
H	tank height [m]
HTF	heat transfer fluid
L_F	heat latent [$J.kg^{-1}$]
Pr	Prandtl number
q	flow rate [$m^3.h^{-1}$]
r	radius of capsules [m]
Ra	Rayleigh number
Re	Reynolds number
t	time [s]
T_f	HTF temperature [°C]
T_{PCM}	PCM temperature [°C]
T_S	maximum value of T_f at the inlet of the tank [°C]
u	velocity [$m.s^{-1}$]
U	heat transfer coefficient [$W.m^2.K^{-1}$]
x	position along the direction of the tank [m]

Greek symbols

β	heating rate (°$C.h^{-1}$)
λ	thermal conductivity [$W.m^{-1}.K^{-1}$]
ρ	fluid density [$kg.m^{-3}$]
μ	dynamic viscosity [Pa.s]
ε	porosity

Subscripts

eff	effective
f	fluid
ini	initial
l	liquid state of PCM
m	melting
pcm	phase change material
s	solid state of PCM

1. Introduction

Energy storage represents a promising challenge in the energy transition, both in terms of optimising the performances of energy resources and promoting access to them [1-2]. Indeed, making possible to adjust the "production" and "consumption" of energy while limiting losses [3]. Energy is stored when its availability is greater than needs, and can be recuperated when demand is higher [4]. Given the intermittent or fluctuating production of certain types of energy, such as renewable energies, this operation also makes it possible to meet a constant demand [5]. The thermal energy storage systems are among the options that can address this challenge [6-7]. For example, in France, the thermal storage provides important services to the electrical system and increases the flexibility of the power grid. Many thermal storage options are currently mature or under development and are used in the residential sector (i.e. domestic hot water tanks), in district heating and cooling systems, to recuperate waste heat in industry or to optimize the production of solar thermodynamic power plants [8]. With the development of district heating and cooling systems, massive thermal storage could play an increasing role [9]. Three approaches can be envisaged for thermal energy storage: sensible heat storage, latent heat storage and thermochemical heat storage. Sensitive heat storage is the most mature technology but it has lowest energy density, followed by latent storage and then thermochemical storage [10].

Latent heat storage using Phase Change Materials (PCMs) is recognized as one of the most attractive energy storage techniques, due to its high-energy storage density and capacity to deliver constant temperature performance [11–13]. It can be used for electrical load management in various applications by displacing electrical heating and cooling needs from peak to off-peak times [14]. Among the most important applications of latent heat storage systems are air conditioning and thermal comfort (4 to 20 °C) and the medical and food sectors (-20 to 10 °C) [15-16]. Cold storage using PCMs permits to save a considerable amount of energy and to increase the lifetime of the cooling units [8,17]. Different technologies can be used to store cold in latent energy form [11]. Packed-bed heat storage based on PCM is among the technologies that have been tested and used in recent years in the medical and food industries for cold storage [17]. Such systems are generally cylindrical tanks filled with spherical capsules of PCMs that allow the storage of large amounts of energy by latent heat. These systems contain a fixed bed of spherical capsules of PCM, which is traversed by a heat transfer fluid in order to carry out thermal charging or discharging by

convective heat transfer [18-19]. Several models have been developed to simulate the dynamic and thermal behaviour of heat storage systems [20–22]. There are two main groups of numerical models: the homogeneous model and the heterogeneous model [23]. The first one (homogeneous model) considers the PCM and the HTF as an equivalent homogeneous medium with a unique local temperature. The second model takes into account the thermal gradient between the PCM and the heat transfer fluid. In general, the use of the homogeneous model is justified by the small size of the spherical capsules and the low flow velocity of the HTF [24-25].

There are three types of heterogeneous model: the Schumann model [26], the concentric diffusion model [27], and the continuous solid phase model [28]. The Schumann model is one-dimensional and takes into account the heat transfer between the HTF and the PCM [26]. However, this model has its limits since it does not take into consideration the axial heat conduction within the fluid and the PCM, as well as radial diffusion within the spherical PCM capsule [29]. The concentric diffusion model is a heterogeneous two-phase model, which has the specificity of accounting for thermal conduction within the PCM and the heat transfer between the HTF and the spherical PCM capsule [30-31]. This model considers the bed of capsules as an isotropic porous medium and divides it into several layers in the axial direction. All the spherical capsules in the same layer are assumed to behave in the same manner and each layer can be modelled and discretized using a single spherical capsule [32-33]. The continuous solid phase model considers the latent storage system as a continuous medium and not as a medium composed of independent PCM capsules. However, conduction in axial (one-dimensional model) and/or radial (two-dimensional model) directions within the PCM medium can be considered [34]. There are two coupled expressions in the system of energy conservation equations, one for the PCM and one for the HTF [35-36].

To the best of our knowledge, few numerical studies have been published on positive latent cold storage utilizing PCM having a melting temperature between 0 and 4°C. This work aims to present a mathematical model to describe the performance of a cold energy storage tank using PCMs confined in spherical capsules. The PCMs studied range in phase change temperatures from 0°C to 4°C and the solution of monoethylene glycol is used as heat transfer fluid (HTF).

A detailed study was also carried out to better understand the behaviour of latent storage using multiple PCMs. In this paper, a heat source method [37], which is different from the models discussed above, is used as the physical model to describe the phase change process inside the

capsules. This method has the particularity of taking into account the thermal conduction during the melting process of PCM as well as the natural convection in the liquid phase of the PCM via an effective thermal conductivity.

2. Physical model

In the industry, most of the cold storage tanks are installed in vertical position (see **Fig.1**), where the HTF circulates from the bottom to the top during the charge period and from the top to the bottom during the discharge period. This mode of storage allows a good stratification of the flow during charging and discharging phases.

Fig.1: Cold storage systems [38]

The principal hypotheses used to describe the flow and heat transfer involving phase change in the tank are as follows:

- The packed bed is vertical and well insulated.
- To ensure a good stratification in the tank, the flow is carried out from the top to the bottom during discharge period.

- The flow in the tank is unidirectional and the phase change in the capsules is considered concentric according to the radius of the capsule.
- All capsules have the same diameter (d).
- In each control volume, all capsules are assumed to have the same thermal behaviour.

Under these assumptions, the energy conservation equations in each control volume (see **Fig.2**) can be written as:

➢ ***For HTF***:

$$\rho_f c_f \varepsilon \frac{\partial T_f}{\partial t} + \rho_f c_f u_f \frac{\partial T_f(x,t)}{\partial x} = \lambda_f \frac{\partial^2 T_f(x,t)}{\partial x^2} + U_f A_f \left(T_{pcm}(r=\frac{d}{2}) - T_f(x,t) \right) \quad \textbf{(1)}$$

where, T_f is the HTF temperature, c_f is the specific heat capacity of the HTF, ρ_f is its density and ε is the porosity of the packed bed.

➢ ***For PCM***:

$$(\rho c)_{pcm} \frac{\partial T_{pcm}(r,t)}{\partial t} = \frac{1}{r^2} \frac{\partial}{\partial r} \left(r^2 \lambda_{pcm} \frac{\partial T_{pcm}(r,t)}{\partial r} \right) - \rho_{pcm} L_F \frac{\partial f(r,t)}{\partial t}$$

(2)

where, L_F is the heat of latent melting, f is the liquid fraction and $(\rho c)_{pcm}$ and λ_{pcm} can be calculated by the following expressions :

$$(\rho c)_{pcm} = \rho_{pcm} \left[(1-f) c^s_{pcm} + f\ c^l_{pcm} \right] \quad \textbf{(3)}$$

$$\lambda_{pcm} = (1-f) \lambda^s_{pcm} + f\ \lambda^l_{eff,pcm} \quad \textbf{(4)}$$

The correlation proposed by Lacroix [39] is adopted to determine the effective thermal conductivity $\lambda^l_{eff,pcm}$ of the PCM at the liquid state by considering the effects of natural convection during melting process :

$$\lambda^l_{eff,pcm} = a.Ra^b.\lambda^l_{pcm}$$

(5)

where, *a* and *b* are constants and equal to 0.05 and 0.5, respectively. The Rayleigh number Ra is computed using the following expression:

$$Ra = \left(\beta \; g \left(\rho c \right)_{pcm}^{l} d^{3} \left| T_f - T_m \right| / \left(\mu_{pcm}^{l} \lambda_{pcm}^{l} \right) \right) \quad \textbf{(5)}$$

where, g is the gravitational acceleration, β is the PCM thermal expansion coefficient, μ_{pcm}^{l} is the dynamic viscosity of the liquid PCM and T_m is the melting temperature of the PCM. The heat transfer coefficient U_f can be determined by using the correlation proposed by Beek [40]:

$$U_f = \frac{\lambda_f}{d} \left[3.22 \, \mathrm{Re}^{1/3} \, \mathrm{Pr}^{1/3} + 0.117 \, \mathrm{Re}^{0.8} \, \mathrm{Pr}^{0.8} \right] \quad \textbf{(6)}$$

The superficial capsule area per unit tank volume can be calculated by using the following expression:

$$A_f = \frac{6\left(1-\varepsilon\right)}{d} \quad \textbf{(7)}$$

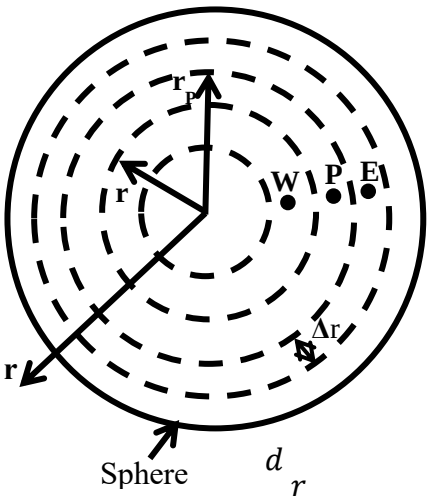

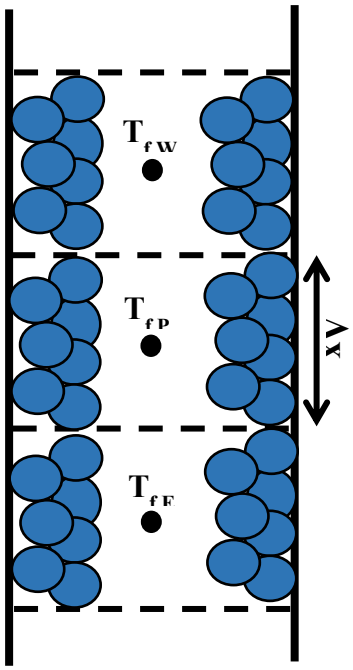

Fig.2: Discretisation of a PCM capsule and the tank

The initial and boundary conditions are chosen as follows:

- ***For heat transfer fluid:***

$$T_f(x,0) = T_{ini}; \quad T_f(0,t) = \beta_1 t + T_{ini}; \quad \frac{\partial T_f(L,t)}{dx} = 0 \tag{8}$$

- ***For PCM:***

$$T_{pcm}(r,0) = T_{ini}; \ \frac{\partial T(0,t)}{\partial r} = 0; \ -\lambda_{pcm}\frac{\partial T_{pcm}}{\partial r} = U_f\left(T_{pcm} - T_f\right) at \ r = \frac{d}{2} \tag{9}$$

A fully implicit finite volume method was used to solve the energy equations system. The first-order upwind scheme was applied to address convective terms, and diffusion terms are discretized using the second order of the central differential scheme**.** Therefore, the resulting expression of the system of energy equations is given as follows:

- ***HTF***

$$a_{f,P}T_{f,P} = a_{f,W}T_{f,W} + a_{f,E}T_{f,E} + a^0_{f,P}T^0_{f,P} + b_f \tag{10}$$

With :

$$a_{f,P} = a_{f,W} + a_{f,E} + U_f A_f \Delta x \tag{11}$$

$$a_{f,\mathrm{W}} = \frac{\lambda_f}{\Delta x} + \varepsilon\rho_f c_f \frac{u}{2}; \ a_{f,\mathrm{E}} = \frac{\lambda_f}{\Delta x} - \varepsilon\rho_f c_f \frac{u}{2}; \ b_f = U_f A_f T_{pcm}\left(\frac{d}{2}, t\right) \tag{12}$$

➢ ***PCM***

$$a_{\mathrm{pcm},P}T_{\mathrm{pcm},P} = a_{\mathrm{pcm},W}T_{\mathrm{pcm},W} + a_{\mathrm{pcm},E}T_{\mathrm{pcm},E} + a^{0}_{\mathrm{pcm},P}T^{0}_{\mathrm{pcm},P} + b_{pcm} \quad \textbf{(13)}$$

With :

$$a_{\mathrm{pcm},P} = a^{0}_{pcm,P} + a_{pcm,\mathrm{W}} + a_{pcm,\mathrm{E}}$$

(14)

$$a^{0}_{pcm} = \rho_{pcm}c_{pcm}\left(\frac{r_E^2 - r_W^2}{3\Delta t}\right); a_{pcm,W} = \frac{r_W^2\lambda_{pcm,W}}{\Delta r}; a_{pcm,\mathrm{E}} = \frac{r_E^2\lambda_{pcm,\mathrm{E}}}{\Delta r} \quad \textbf{(15)}$$

$$b_{pcm} = \rho_{pcm}L_F\left(\frac{r_E^3 - r_W^3}{3\Delta t}\right)\left(f_P(t) - f_P(t+\Delta t)\right)$$

(16)

where *E* and *W* represents the East and West of each control volume. r_E and r_W refer to the local radius of the P control volume faces. In this paper, **Eqs. 10** and **13** were solved iteratively by using a Tridiagonal Matrix Algorithm (TDMA) method [41]. The computation procedure was carried out using Fortan 90. The specified iteration in each time interval was considered convergent when the maximum relative residual of T_f *and* T_{pcm} was less than 10^{-4}. During this iterative process, the liquid fraction was updated, at each iteration, using Swaminathan and Voller method [42]:

$$f_P^{k+1}(t) = f_P^{k}(t) + \frac{a^{k}_{pcm,P}}{\rho^{k}_{pcm}L_F}\left(T^{k}_{pcm,P} - T_m\right) \quad \textbf{(17)}$$

where, index k refer to the newest iteration loop. The liquid fraction is corrected at each control volume using the following test

$$f_P^{k+1} = \begin{cases} 0 & if \quad f_P^{k+1} \le 0 \\ 1 & if \quad f_P^{k+1} \ge 1 \end{cases}$$

(18)

3. Physical model validation

The different PCMs considered in the present study are labelled PCMi where i corresponds to the value of their melting temperature. Two studies were selected from the literature to validate our physical model. The first one **[43]** consists in studying the discharge phase (melting process) in a cylindrical tank filled with spherical capsules containing ice as a PCM. The second one **[36]** consists in studying the melting process in a system containing three PCMs confined in spherical capsules and placed successively in a cylindrical tank.

3.1 Melting process in a cylindrical tank filler with spherical capsules containing ice

In this study **[43]**, the flow rate of the HTF varies between $1 m^3.h^{-1}$ and $2.3\ m^3.h^{-1}$ and the maximum temperature of the HTF at the inlet of the tank ranges between 4°C and 10°C. The storage tank, which was studied by Bedecarrats et al. **[43-44]** and Kousksou et al. **[45-46]** contains approximately 2500 spherical capsules containing water as PCM and with a diameter of d = 77 mm. The useful height of the tank is H = 1.42 m and its internal diameter is D = 0.94 m. The tank is insulated with polyurethane foam and it is initially at temperature T_o lower than the melting temperature of ice (in our case T_o = -6°C). During the discharging phase (melting process), the temperature of the heat transfer fluid (solution of monoethylene glycol) at the inlet of the tank increases continuously until it reaches a maximum value called the final inlet temperature T_s (in our case +6°C) and remains at this temperature until the end of discharge mode. The heat transfer fluid flows from the top to the bottom of the tank. We assumed that the instant at which the temperature at the exit of the stock reaches that of the inlet corresponds to the end of the discharge process.

Fig.3 illustrates the temperature evolution of the HTF at the outlet of the tank for three flow rates. The same temperature was imposed at the inlet of the tank for those three flow rates. On the same figure, we presented the experimental temperatures of the HTF at the outlet of the tank, which are obtained by Bedecarrats et al. **[43-44]**. It is clear that the duration of the discharge decreases by increasing the flow rate. This may be explained by the fact that the increase in flow rate leads to an increase in heat transfer between the heat transfer fluid and the capsules. Also, we can observe that the numerical results are in good agreement with the experimental data. The slight difference between the numerical and experimental results can be explained by the following points:

- According to experimental observations **[43]**, the melting process begins uniformly on the inner surface of the capsule shell. In the case of water, as soon as the amount of liquid is sufficient, the gravitational forces due to the difference density between the

solid and liquid phases push the ice up against the top wall of the capsule. This process can accelerate the melting inside the capsule. In our model, this phenomenon has been neglected.

- In our model, heat exchanges between the tank and the ambient air are neglected. These heat exchanges with the ambient air may slightly heat up the HTF and impact the melting process inside the capsules.

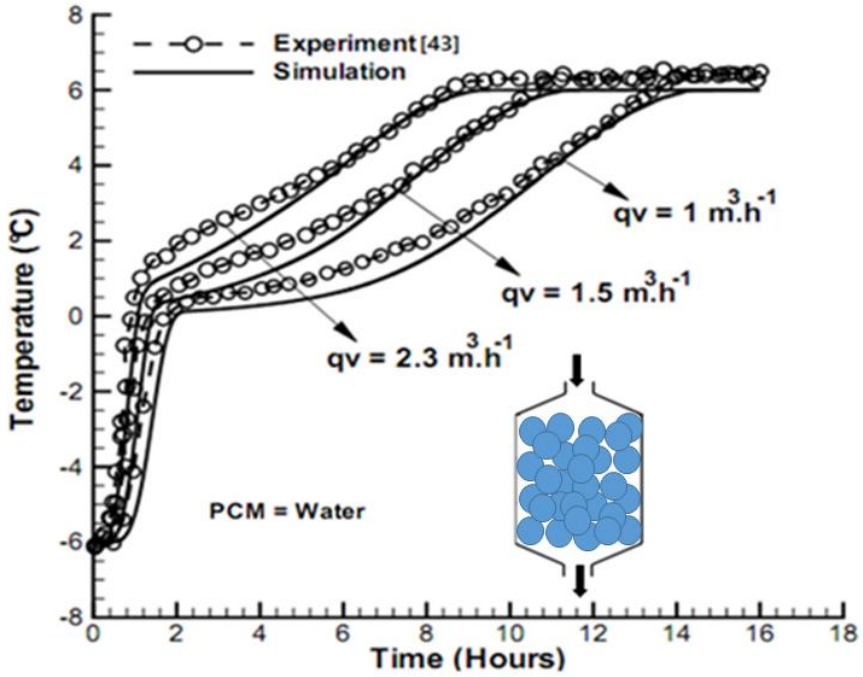

Fig.3: Variation in HTF temperature versus time at the outlet of the tank for different flow rates

3.2 Melting process in a cylindrical tank filled with three PCMs

In this work **[36]**, a packed bed heat storage system (diameter = 0.36 m and height = 0.46 m) containing spherical capsules (diameter = 55 mm) confining three types of PCMs was numerically studied. The apparent heat capacity method is used by the authors [36] to describe the melting process inside the PCM. The capsules are placed in series according to the melting temperature of the PCM (see **Table 1** and **Fig.4**). Water is used as a HTF and heated in the solar collector. The flow rate is 2 L/min and the initial temperature of the HTF

and PCMs is 26°C. The inlet water temperature of the tank has been determined using the same methodology reported by Yang et al. **[36]**.

Fig.4 presents the temperature evolution of the HTF and the PCM at various positions inside the tank. A good agreement was found between our numerical HTF temperatures and those obtained by Yang et al. **[36]**. However, a difference between the two results was observed for PCM temperatures especially during the three stages indicating the phase change process. This discrepancy can be explained by the fact that Yang et al. **[36]** used the apparent heat capacity method to investigate the melting in PCMs while in our model we employed the heat source method. It is interesting to recall that with the apparent heat capacity method, the phase change is supposed to be performed over a temperature range while with the heat source method the fusion is carried out at constant temperature (i.e.the melting temperature).

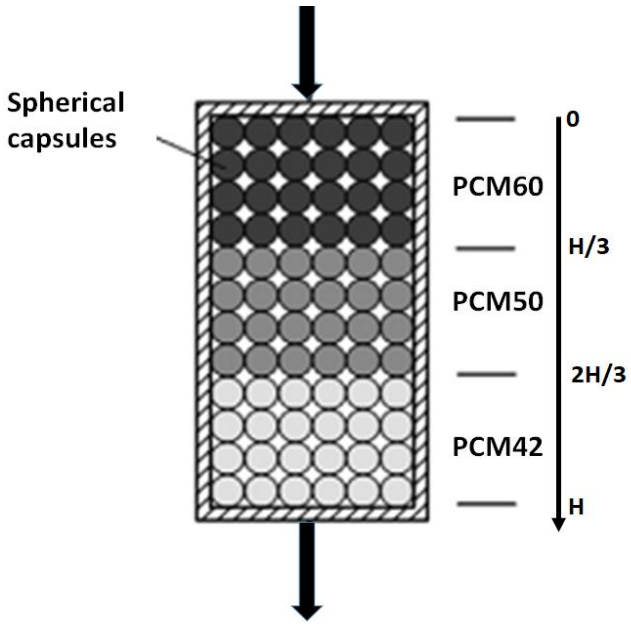

Fig.4: Schematic diagram of the tank with multi PCMs

Table 1: Properties of the PCMs considered **[36]**

	PCM60	**PCM50**	**PCM42**
Density ($kg.m^{-3}$)			
Solid	861	848	844
Liquid	778	767	760
Latent heat ($kJ.kg^{-1}$)	209	200	168

Melting temperature (°C)	60	50	42
Specific heat capacity ($J.kg^{-1}.K^{-1}$)			
Solid	1850	1650	2052
Liquid	2384	1863	2411
Thermal conductivity ($W.m^{-1}.K^{-1}$)			
Solid	0.4	0.4	0.4
Liquid	0.15	0.15	0.15

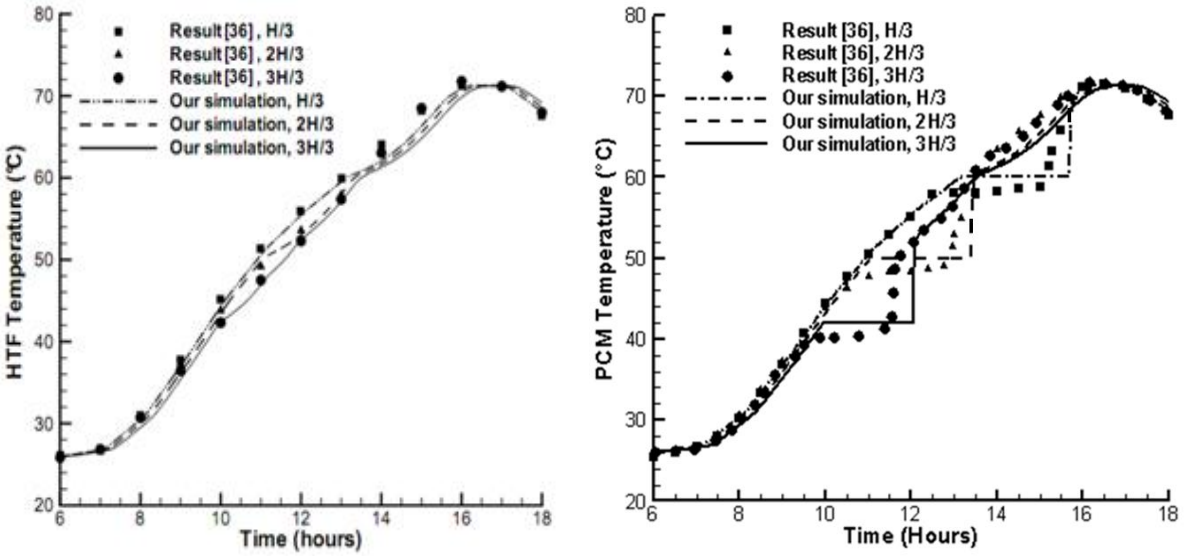

(a) (b)

Fig.5: Variation in HTF temperature (a) and PCM temperature (b) versus time at various positions inside the tank

4. Results and discussion

The list of the main properties of the PCMs studied in this section is presented in **Table 2**. In the following of this work, the dimensions and characteristics of the tank studied by Bedecarrats et al. **[43-44]** are used in the numerical simulations.

Table 2: Main properties of the PCMs considered **[47]**

	PCM0	**PCM2**	**PCM4**
Density ($kg.m^{-3}$)			
Solid	917	888	880
Liquid	1000	777	760

Latent heat (kJ.kg^{-1})	333	200	180
Melting temperature (°C)	0	2	4
Specific heat capacity (J.kg^{-1}.K^{-1})			
Solid	2040	1980	1990
Liquid	4220	2000	2005
Thermal conductivity (W.m^{-1}.K^{-1})			
Solid	2.25	0.2	0.2
Liquid	0.6	0.18	0.19

4.1 Single-type packed bed PCM storage tank

Fig.6 shows the numerical temperature of the HTF as a function of time between the inlet and outlet of the tank. The flow rate q_v of the HTF is equal to 1 m^3.h^{-1}. It can be noticed that the temperature of the HTF in the control volumes that are close to the inlet of the tank does not display a significant plateau during the melting process inside the capsules. One can conclude that the phase change within the capsules in these control volumes occurs relatively rapidly. However, the temperature of the HTF in the control volumes close to the exit of the tank shows a noticeable plateau while the phase change in the capsules is taking place. We can note that the temperature of the HTF at the outlet of the tank over the early stages of the discharge mode remains practically constant. This period corresponds to the time required (i.e. residence time) for the HTF to reach the outlet of the tank. The analysis of this curve indicates also that there is a stratification in the tank and the flow in the system corresponding to a piston flow.

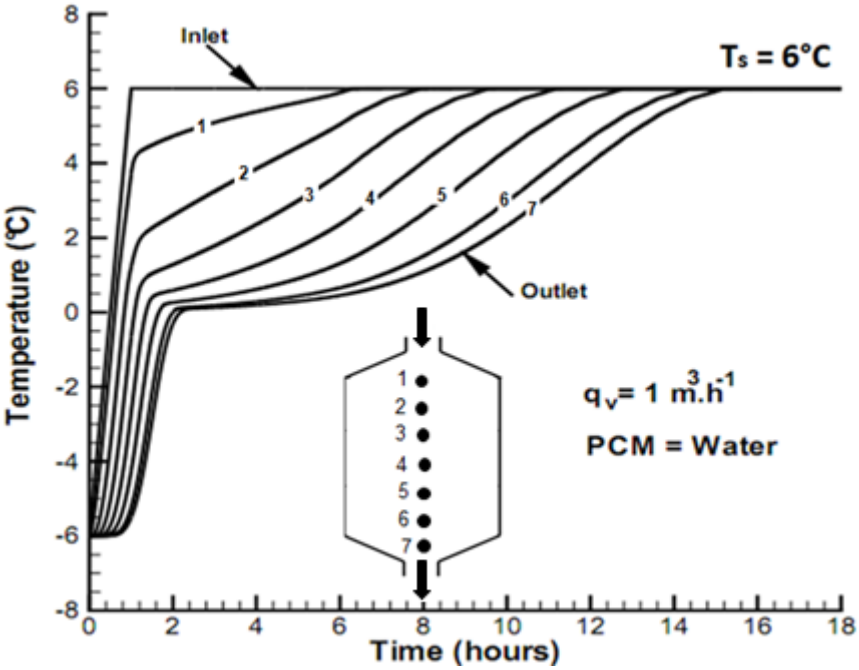

Fig.6: Variation in heat transfer fluid temperature from inlet to outlet of the tank

Using the physical model, it is possible to determine the amount of PCM melted (i.e. the liquid fraction) in the capsules during the discharge mode (See **Fig.7**). This parameter allows us to easily detect the beginning of melting process in the capsules as well as the end of latent storage in the tank. Therefore, we can determine the latent storage time in the tank.

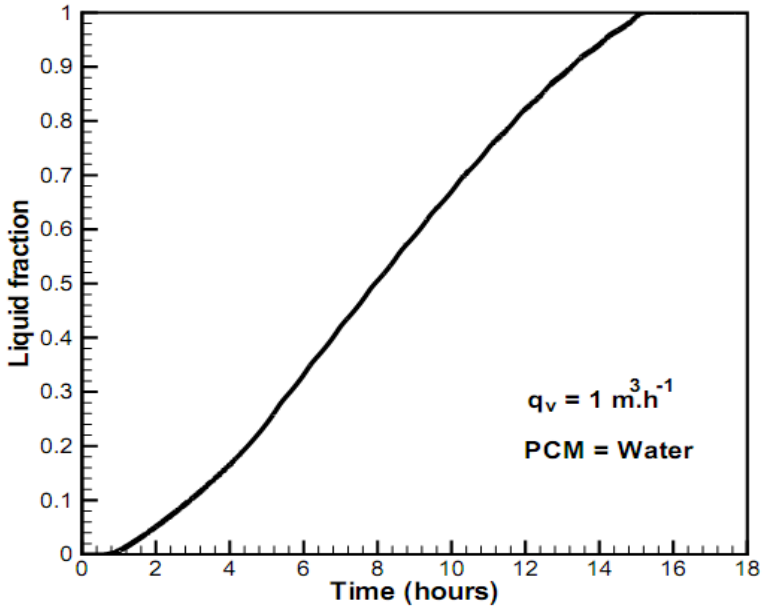

Fig.7: Liquid fraction of PCM versus time inside the tank

Fig.8 presents the temperature evolution of the HTF at the outlet of the tank as a function of time and for different temperatures Ts. it is remarked that the time of discharge is reduced by

increasing Ts. These results are evident, since the higher temperature level at the inlet of the tank accelerates the phase change process inside the capsules and reduces the time required for the PCM to melt in the tank.

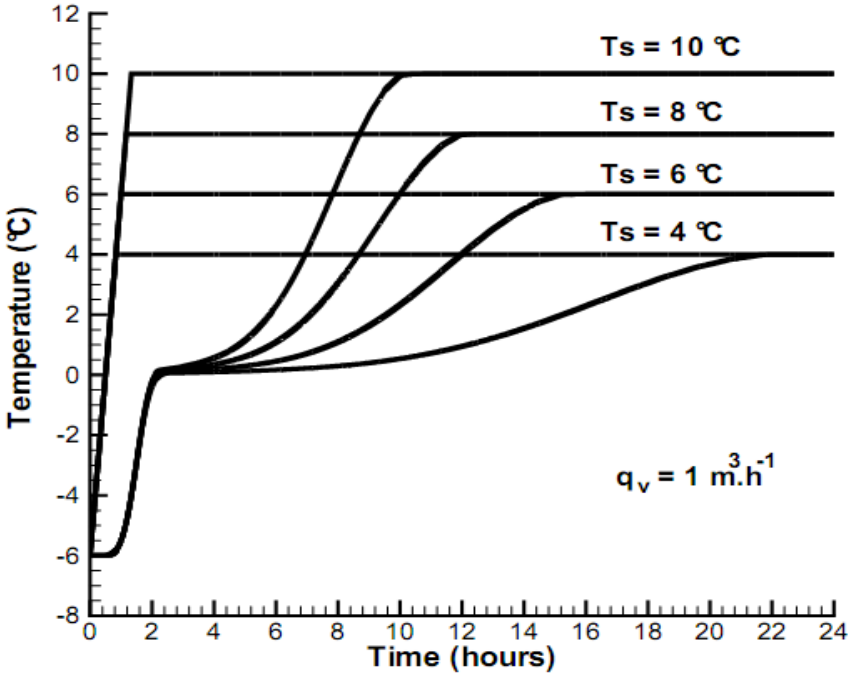

Fig.8: Variation in HTF temperature versus time at the outlet of the tank for different final inlet temperatures T_s

Fig.9-a illustrates the effect of capsule diameter on the energy performance of the tank. The reduction in the capsule diameter leads to an increase in the number of capsules and therefore the exchange surface between the HTF and the PCM. The discharge time is reduced by decreasing the diameter of the capsules. For the three diameters considered, the latent energy of the PCM was fully recuperated.

It is clearly observed in **Fig.9-b** that an increase in tank size leads to an increase in d the discharge time. It is also shown that the larger the size of the tank, the greater the plateau in the outlet temperature of the storage tank. This plateau represents the solid-liquid phase change process inside the capsules.

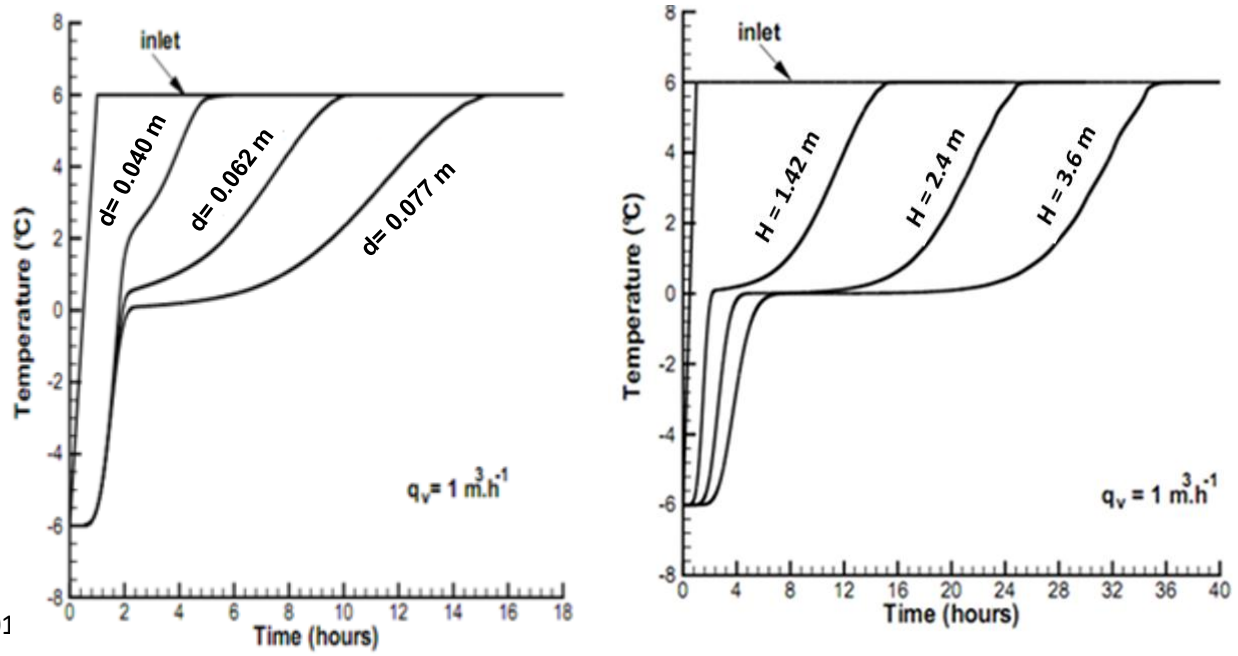

(a) (b)

Fig.9: Variation in HTF temperature versus time at the outlet of the tank for different diameter of capsule **(a)** and for various volumes of the tank **(b)**

Two parrafins (PCM2 and PCM4) were selected to examine the influence of the melting temperature on the thermal performances of the latent storage system (see **Table 1**). **Fig.10** illustrates the effect of the phase change temperature on the discharge time. On this figure, the evolution of the HTF temperature is presented as a function of time between the inlet and outlet of the tank. One can see that the discharge time increases significantly as melting temperature of the PCM approaches the temperature T_S. These results can be explained by the fact that when the fusion temperature of the PCM is close to the maximum temperature reached by the HTF temperature at the inlet of the tank, the rate of transfer between the fluid and the capsules decreases which slows the process of melting inside the tank.

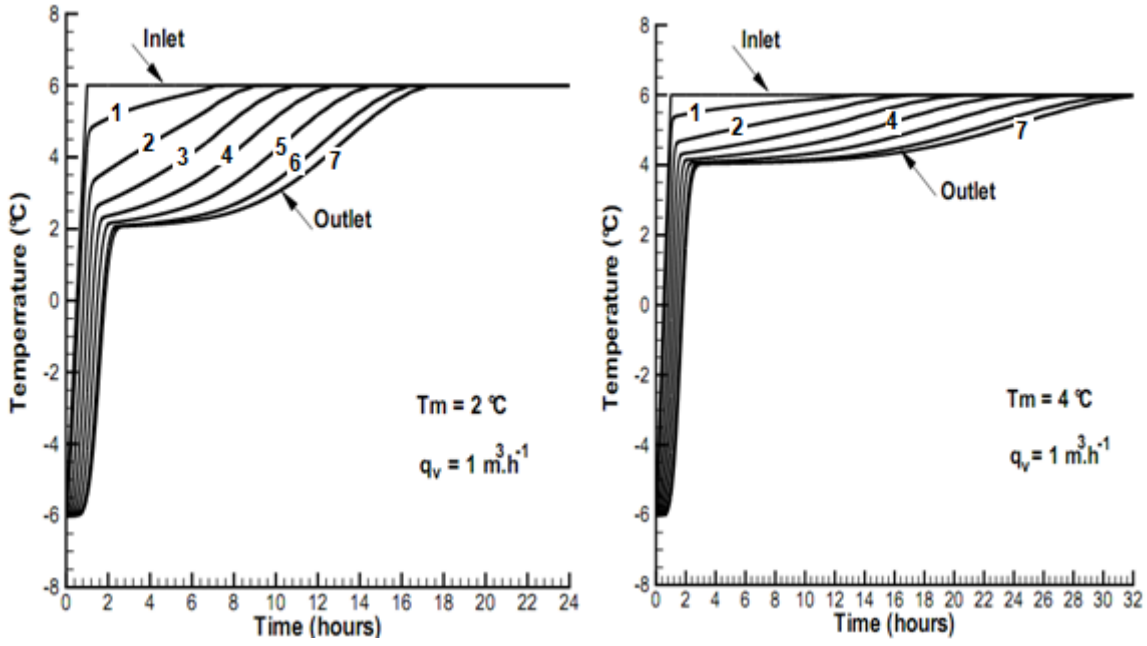

(a) **(b)**

Fig.10: Effect of melting temperature on the thermal performance of storage system **(a)** T_m = 2°C - **(b)** T_m = 4°C.

The principal objective of a thermal energy storage system is to ensure a good heat transfer efficiency during discharging process with an acceptable pumping imperative. The Ergun equation [47] is used to determine the pressure drop through packed beds of spherical capsules:

$$\frac{\Delta p}{H} = A\frac{(1-\varepsilon)^2}{\varepsilon^3}\frac{\mu_f . u_e}{d^2} + B\frac{(1-\varepsilon)}{\varepsilon^3}\frac{\rho_f u_e^2}{d} \quad (19)$$

Where μ_f is the dynamique viscosity of the HTF, u_e is the superficial bed velocity (i.e. the average velocity of the HTF in an empty bed), ρ_f is the density of the HTF, A is 150 and B is 1.75. The first term on the right-hand side refers to the viscous energy losses that govern during laminar flow and the second term accounts for kinetic losses that dominate in the turbulent regime.

Fig.11 illustrates the pressure drop across the packed bed for various values of HTF flowrate and for different diameter of the spherical capsule. The analysis of this figure shows that, in

general, for a relatively small values of the flow rate of the HTF, the use of spherical capsules with a large diameter can be beneficial in terms of thermal packing bed efficiency and pumping performance.

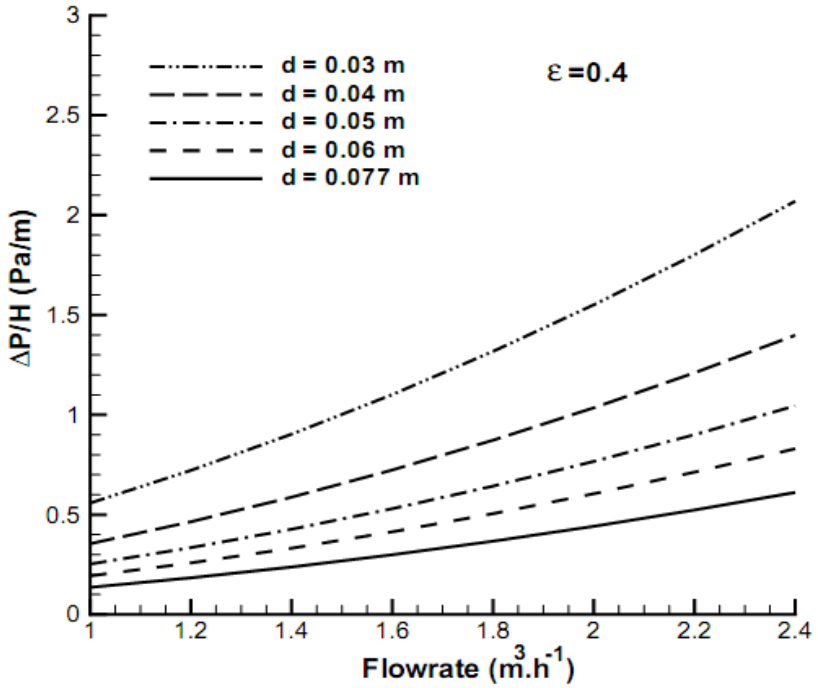

Fig.11: Variation of pressure drop with flowrate of HTF for various values of spherical capsule diameter

4.2 Multiple-type packed bed PCM storage tank

Recent methods used to improve the efficiency of latent storage systems involve the use of different materials in cascade mode. The cascade mode, which uses several PCMs permits to improve the charge and discharge rate during phase change period [48]. This method ensures an uniform and stable HTF temperature at the outlet of the tank for a prolonged period of time [49–51]. It also leads to higher the energy capacity and the exergy efficiency of the system [52–54]. Considering the advantages of these storage systems, a cascading positive cold storage system with multiple PCMs may also be attractive and potentially preferable to a single PCM cold storage system. In the continuation of this work, we placed three PCMs (see **Table 2**) in series in the storage system. The three PCMs occupy the same volume in the tank (see **Fig.12**).

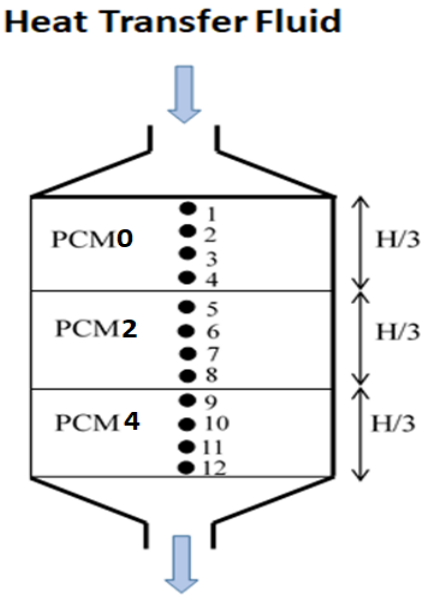

Fig.12: Cascade latent storage system

In **Fig.13**, we presented the evolution of the temperature of the heat transfer fluid between the inlet and the outlet of the tank for different location of the PCMs in the tank. Six configurations were studied and analysed. All configurations tested received the same flow rate and HTF temperature profile at the inlet of the tank. The analysis of **Fig.13** shows that the performance of the storage tank depends essentially on the location of the PCMs in the tank. It is interesting to note that when PCMs are placed in series and in ascending order of melting temperature: the PCM with the low melting temperature (T_m=0°C) is heated from T_{in} = -6°C to T=2°C. The PCM with the medium melting temperature (T_m = 2°C) is heated from T = 0°C to T=4°C and the PCM with the high melting temperature (T_m = 4°C) is heated from T=2°C to the maximum temperature T_S = 6°C. With this configuration, PCMs lose only a small amount of storage density as the temperature ranges for latent heat storage are completely exploited. In reality, this operating scenario is applicable only in certain cases. For example, when the time discharge for single PCM system is too short; the PCM may not be fully utilized for latent heat storage (see **Fig.10-b**). With a cascade storage, this problem can be solved. We can also note that the HTF temperature profile at the outlet of the tank is strongly influenced by the arrangement of PCMs inside the tank. For all configurations, the flow in the tank is a piston flow from top to bottom. The discharge time can be significantly reduced according to the distribution of the PCMs in the tank.

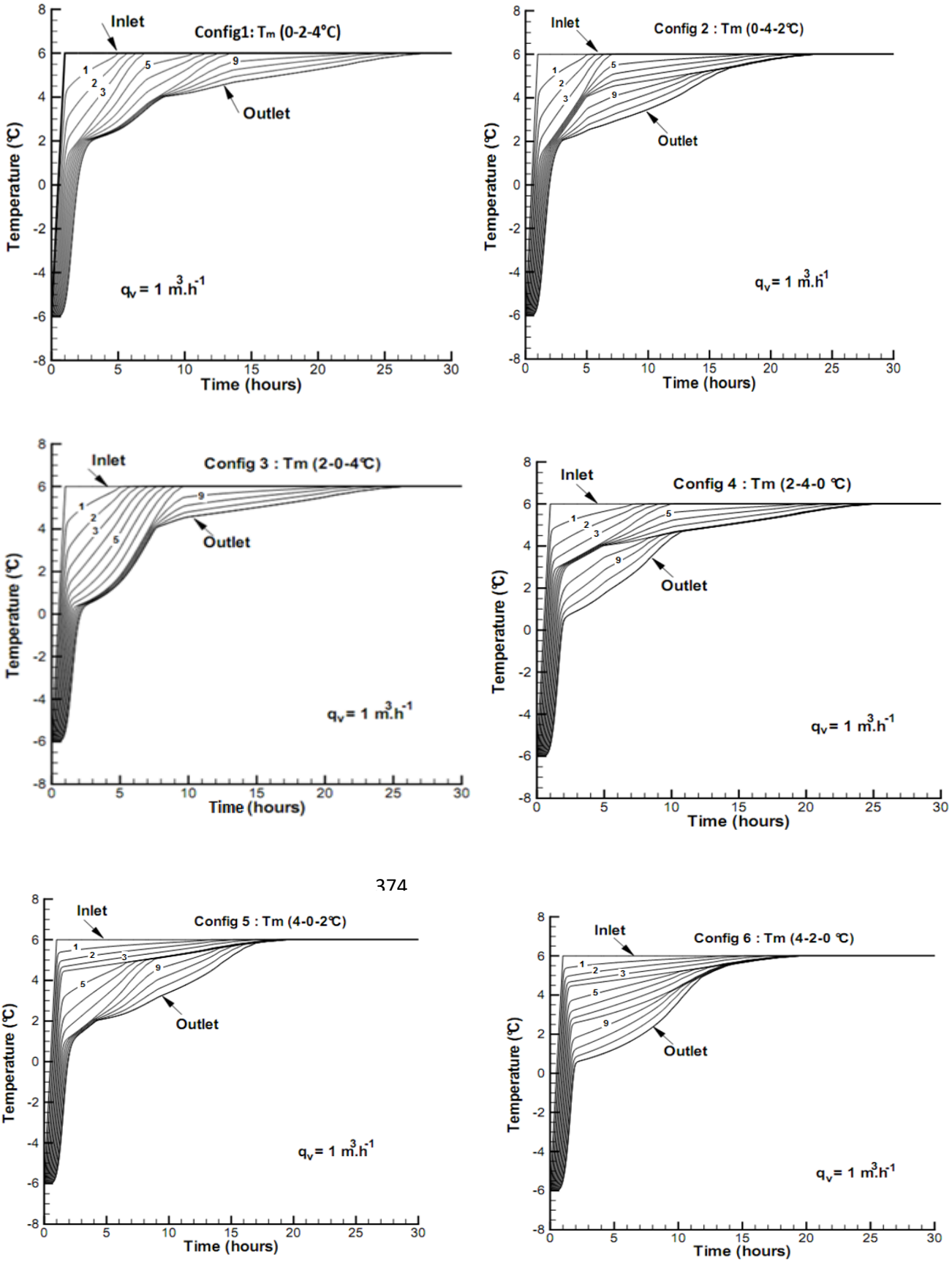

372

373

374

381

382 **Fig.13:** Latent storage system using three PCMs in series

In **Fig.14**, we presented the influence of the flow rate and inlet HTF temperature on the thermal performance of the cascade system for configuration 1 (T_m = 0→2→4°C). Similarly, to a latent storage system with a single PCM, the discharge time is reduced by increasing the HTF flow rate and temperature Ts at the inlet of the tank. These results can be explained by the fact that the increase in flow rate and Ts intensifies the heat transfers between the fluid and the capsules, therefore accelerating the melting process in the capsules.

To conclude, the thermal behaviour of the cascade mode depends on several parameters such as the arrangement of the PCMs inside the tank, the discharge time, the flow rate and the HTF temperature profile at the inlet of the tank. Therefore, it is necessary to use a multi-criteria approach to optimise the energy performance of the system in cascade mode.

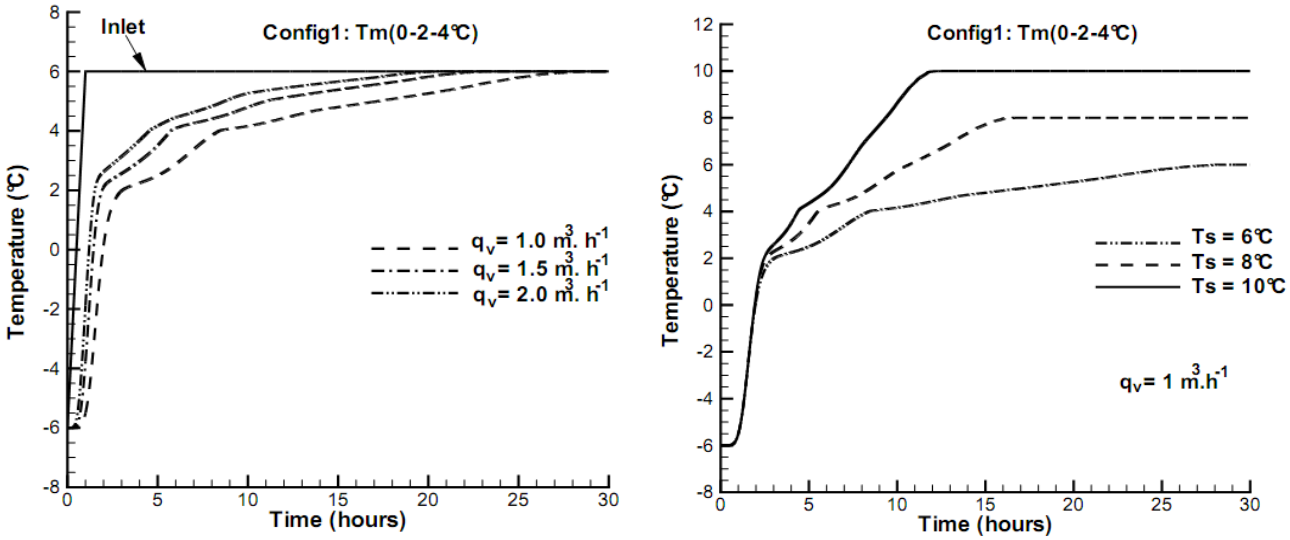

(a) **(b)**

Fig.14: The effect of flow rate **(a)** and Ts **(b)** on the outlet HTF temperature of the cascade system.

5. Conclusion

A physical model has been developed to describe the energy performance of a latent storage tank during the discharge period. The storage system consists of a tank with a fixed bed of phase-change materials. The numerical model have been validated using experimental data from literature. The effects of HTF temperature at the inlet of the tank, HTF flow rate

and melting temperature of the PCM on the thermal performance of latent storage system were presented and discussed. Higher inlet HTF temperature resulted in higher content of the stored energy as well as lower discharging required time. The increase in HTF flowrate, resulted in higher overall heat transfer and lower charging time. The discharge time increases significantly as the melting temperature of the PCM approaches the temperature T_S. A comprehensive study was also performed to understand the behaviour of the latent storage system using multiple PCMs. It is found that the thermal behaviour of the multi-PCM configuration depends on the placement order of the PCMs inside the tank, the flow rate of the HTF and the level temperature of the HTF at the inlet to the tank. As a perspective, a work is in progress to optimize the energy performance of multiple PCMs system during the charge and discharge periods by using the exergetic approach. Another model is under development to incorporate several PCMs inside the same capsule.

References

[1] C. Prieto, L.F. Cabeza, Thermal energy storage (TES) with phase change materials (PCM) in solar power plants (CSP). Concept and plant performance, Appl. Energy. 254 (2019) 113646.

[2] H. Zhang, J. Baeyens, G. Caceres, J. Degreve, Y. Lv, Thermal energy storage: Recent developments and practical aspects, Prog. Energy Combust. Sci. 53 (2016) 1–40.

[3] J. Gasia, D. Groulx, N.H.S. Tay, L.F. Cabeza, Numerical study of dynamic melting enhancement in a latent heat thermal energy storage system, J. Energy Storage. 31 (2020) 101664.

[4] H. Liang, J. Niu, Y. Gan, Performance optimization for shell-and-tube PCM thermal energy storage, J. Energy Storage. 30 (2020) 101421.

[5] M. Müller, L. Viernstein, C.N. Truong, A. Eiting, H.C. Hesse, R. Witzmann, A. Jossen, Evaluation of grid-level adaptability for stationary battery energy storage system applications in Europe, J. Energy Storage. 9 (2017) 1–11.

[6] E. Guelpa, V. Verda, Thermal energy storage in district heating and cooling systems: A review, Appl. Energy. 252 (2019) 113474.

[7] Y. Chaibi, T. El Rhafiki, R. Simón-Allué, I. Guedea, S.C. Luaces, O.C. Gajate, T. Kousksou, Y. Zeraouli, Air-based hybrid Photovoltaic/Thermal systems: A review Y., J. Clean. Prod. (2021). doi:10.1016/j.jclepro.2021.126211.

[8] B. Nie, A. Palacios, B. Zou, J. Liu, T. Zhang, Y. Li, Review on phase change materials for cold thermal energy storage applications, Renew. Sustain. Energy Rev. 134 (2020) 110340.

[9] S.J. Cox, D. Kim, H. Cho, P. Mago, Real time optimal control of district cooling system with thermal energy storage using neural networks, Appl. Energy. 238 (2019)

466–480.

[10] C. Prieto, P. Cooper, A.I. Fernández, L.F. Cabeza, Review of technology: Thermochemical energy storage for concentrated solar power plants, Renew. Sustain. Energy Rev. 60 (2016) 909–929.

[11] E. Oró, A. De Gracia, A. Castell, M.M. Farid, L.F. Cabeza, Review on phase change materials (PCMs) for cold thermal energy storage applications, Appl. Energy. 99 (2012) 513–533.

[12] T. Kousksou, P. Bruel, A. Jamil, T. El Rhafiki, Y. Zeraouli, Energy storage: Applications and challenges, Sol. Energy Mater. Sol. Cells. 120 (2014) 59–80.

[13] S.-F. Li, Z. Liu, X.-J. Wang, A comprehensive review on positive cold energy storage technologies and applications in air conditioning with phase change materials, Appl. Energy. 255 (2019) 113667.

[14] A. Arteconi, N.J. Hewitt, F. Polonara, State of the art of thermal storage for demand-side management, Appl. Energy. 93 (2012) 371–389.

[15] S. Singh, K.K. Gaikwad, Y.S. Lee, Phase change materials for advanced cooling packaging, Environ. Chem. Lett. 16 (2018) 845–859.

[16] J.K. Carson, A.R. East, The cold chain in New Zealand–A review, Int. J. Refrig. 87 (2018) 185–192.

[17] H. Mehling, L.F. Cabeza, Heat and cold storage with PCM, Springer, 2008.

[18] T Kousksou, T. El Rhafiki, A. Arid, E. Schall, Y. Zeraouli, Power, efficiency and irreversibility of latent energy systems. Journal of thermophysics and heat transfer 22 (2008) 234-239.

[19] J. Park, S.H. Choi, S.W. Karng, Cascaded latent thermal energy storage using a charging control method, Energy. 215 (2021) 119166.

[20] A. de Gracia, L.F. Cabeza, Numerical simulation of a PCM packed bed system: a review, Renew. Sustain. Energy Rev. 69 (2017) 1055–1063.

[21] H.A. Zondag, R. De Boer, S.F. Smeding, J. Van Der Kamp, Performance analysis of industrial PCM heat storage lab prototype, J. Energy Storage. 18 (2018) 402–413.

[22] A. Elouali, T. Kousksou, T. El Rhafiki, S. Hamdaoui, M. Mahdaoui, A. Allouhi, Y. Zeraouli, Physical models for packed bed: Sensible heat storage systems, J. Energy Storage. 23 (2019) 69–78.

[23] X. Cheng, X. Zhai, Thermal performance analysis of a cascaded cold storage unit using multiple PCMs, Energy. 143 (2018) 448–457.

[24] K. Nagano, S. Takeda, T. Mochida, K. Shimakura, Thermal characteristics of a direct heat exchange system between granules with phase change material and air, Appl. Therm. Eng. 24 (2004) 2131–2144.

[25] R. Anderson, L. Bates, E. Johnson, J.F. Morris, Packed bed thermal energy storage: A simplified experimentally validated model, J. Energy Storage. 4 (2015) 14–23.

[26] T.E.W. Schumann, Heat transfer: a liquid flowing through a porous prism, J. Franklin Inst. 208 (1929) 405–416.

[27] T.M. Sanderson, G.T. Cunningham, Performance and efficient design of packed bed thermal storage systems. Part 1, Appl. Energy. 50 (1995) 119–132.

[28] A.F. Regin, S.C. Solanki, J.S. Saini, An analysis of a packed bed latent heat thermal energy storage system using PCM capsules: Numerical investigation, Renew. Energy. 34 (2009) 1765–1773.

[29] E. Tumilowicz, C.L. Chan, P. Li, B. Xu, An enthalpy formulation for thermocline with encapsulated PCM thermal storage and benchmark solution using the method of characteristics, Int. J. Heat Mass Transf. 79 (2014) 362–377.

[30] K.A.R. Ismail, J.R. Henrıquez, Numerical and experimental study of spherical capsules packed bed latent heat storage system, Appl. Therm. Eng. 22 (2002) 1705–1716.

[31] H. Peng, H. Dong, X. Ling, Thermal investigation of PCM-based high temperature thermal energy storage in packed bed, Energy Convers. Manag. 81 (2014) 420–427.

[32] T. Kousksou, P. Bruel, Encapsulated phase change material under cyclic pulsed heat load, Int. J. Refrig. 33 (2010) 1648–1656.

[33] J. Wei, Y. Kawaguchi, S. Hirano, H. Takeuchi, Study on a PCM heat storage system for rapid heat supply, Appl. Therm. Eng. 25 (2005) 2903–2920.

[34] S. Bellan, J. Gonzalez-Aguilar, M. Romero, M.M. Rahman, D.Y. Goswami, E.K. Stefanakos, D. Couling, Numerical analysis of charging and discharging performance of a thermal energy storage system with encapsulated phase change material, Appl. Therm. Eng. 71 (2014) 481–500.

[35] C. Arkar, S. Medved, Influence of accuracy of thermal property data of a phase change material on the result of a numerical model of a packed bed latent heat storage with spheres, Thermochim. Acta. 438 (2005) 192–201.

[36] L.Yang, X. Zhang, G. Xu, Thermal performance of a solar storage packed bed using spherical capsules filled with PCM having different melting points. Energy and Buildings 68 (2014) 639–646.

[37] Y. Khattari, H. El-Otmany, T. El Rhafiki, T. Kousksou, A. Ahmed, E. Ben Ghoulam, Physical models to evaluate the performance of impure phase change material dispersed in building materials, J. Energy Storage. 31 (2020) 101661.

[38] Carrier, Cristpia energy systems, (n.d.). http://www.cristopia.com/.

[39] M. Lacroix, Numerical simulation of a shell-and-tube latent heat thermal energy storage unit, Sol. Energy. 50 (1993) 357–367.

[40] J. Beek, Design of packed catalytic reactors, in: Adv. Chem. Eng., Elsevier, 1962: pp. 203–271.

[41] S. Patankar, Numerical heat transfer and fluid flow, Taylor & Francis, 2018.

[42] C.R. Swaminathan, V.R. Voller, Towards a general numerical scheme for solidification systems, Int. J. Heat Mass Transf. 40 (1997) 2859–2868.

[43] J.P. Bedecarrats, F. Strub, B. Falcon, J.P. Dumas, Phase-change thermal energy storage using spherical capsules: performance of a test plant, Int. J. Refrig. 19 (1996) 187–196.

[44] J.-P. Bedecarrats, J. Castaing-Lasvignottes, F. Strub, J.-P. Dumas, Study of a phase

change energy storage using spherical capsules. Part II: Numerical modelling, Energy Convers. Manag. 50 (2009) 2537–2546.

[45] T. Kousksou, J.-P. Bédécarrats, J.-P. Dumas, A. Mimet, Dynamic modelling of the storage of an encapsulated ice tank, Appl. Therm. Eng. 25 (2005) 1534–1548.

[46] T. Kousksou, J.P. Bédécarrats, F. Strub, J. Castaing-Lasvignottes, Numerical simulation of fluid flow and heat transfer in a phase change thermal energy storage, Int. J. Energy Technol. Policy. 6 (2008) 143–158.

[47] RUBITHERM, PHASE CHANGE MATERIAL, (n.d.). https://www.rubitherm.eu/.

[48] J. Theuerkauf, P. Witt, D. Schwesig, Analysis of particle porosity distribution in fixed beds using the discrete element method, Powder Technol. 165 (2006) 92–99.

[49] A.H. Mosaffa, L.G. Farshi, C.A.I. Ferreira, M.A. Rosen, Energy and exergy evaluation of a multiple-PCM thermal storage unit for free cooling applications, Renew. Energy. 68 (2014) 452–458.

[50] Q. Mao, Y. Zhang, Thermal energy storage performance of a three-PCM cascade tank in a high-temperature packed bed system, Renew. Energy. 152 (2020) 110–119.

[51] S. Christopher, K. Parham, A.H. Mosaffa, M.M. Farid, Z. Ma, A.K. Thakur, H. Xu, R. Saidur, A critical review on phase change material energy storage systems with cascaded configurations, J. Clean. Prod. (2020) 124653.

[52] J.N.W. Chiu, V. Martin, Multistage latent heat cold thermal energy storage design analysis, Appl. Energy. 112 (2013) 1438–1445.

[53] S. Nekoonam, R. Ghasempour, Optimization of a solar cascaded phase change slab-plate heat exchanger thermal storage system, J. Energy Storage. (2020) 102005.

[54] H.J. Xu, C.Y. Zhao, Thermal performance of cascaded thermal storage with phase-change materials (PCMs). Part II: Unsteady cases, Int. J. Heat Mass Transf. 106 (2017) 945–957.

[55] T. Kousksou, F. Strub, J.C. Lasvignottes, A. Jamil, J.P. Bedecarrats, Second law analysis of latent thermal storage for solar system, Sol. Energy Mater. Sol. Cells. 91 (2007) 1275–1281.